Synthesis of Dimethyl Oxalate from CO and CH_3ONO on Carbon Nanofiber Supported Palladium Catalysts

Tie-Jun Zhao,[†] De Chen,[‡] Ying-Chun Dai,[†] Wei-Kang Yuan,*[,†] and Anders Holmen[‡]

UNILAB, State Key Laboratory of Chemical Reaction Engineering, East China University of Science and Technology, Shanghai 200237, China, and Department of Chemical Engineering, Norwegian University of Science and Technology, N-7491 Trondheim, Norway

A series of novel palladium catalysts supported on carbon nanofibers of various nanostructures have been prepared, characterized, and tested in gas-phase synthesis of dimethyl oxalate. Significant improvements in both activity and selectivity have been achieved over well-defined carbon nanofiber supported palladium catalysts. Carbon nanofiber produced on 20% $NiFe/Al_2O_3$ (CNF-05) supported palladium catalyst possesses the highest activity, which can be ascribed to the high surface area of the support, relatively weak metal−support interaction, and smaller metal particles. The low metal−support interaction might improve the redox properties of the catalyst, and thus the activity. The functionalization of CNF-05 in air is found to dramatically increase the conversion of methyl nitrite compared to the functionalization in HNO_3.

Introduction

Diesters of oxalic acid are important raw materials for the syntheses of oxalic acid, glycols, intermediates for dyes, and pharmaceuticals and the extraction of noble metals.[1−4] They are commercially produced by means of the dehydrogenation of sodium formate and esterification of oxalic acid. The use of sodium hydroxide and sulfuric acid causes strong corrosion of the equipment and an environmental problem. Therefore, great attention has been given to the development of new environmentally friendly processes. Large efforts have been devoted to developing new active and selective catalysts, since the catalysts play a key role in the processes.

Metal palladium and palladium salts have been used to catalyze many important organic reactions and have thus been employed in various industrial processes. However, it is found that the redox process between Pd(II) and Pd(0) is the crucial step in the oxidative reactions.[5] By this means dimethyl oxalate (DMO) can be synthesized by methyl nitrite and carbon monoxide in the gas phase over palladium catalysts in a temperature range of 80−120 °C and a pressure range of 0.1−0.5 MPa.[4−6] Nitrogen oxide produced as shown in eq 1 participates in the regeneration reaction expressed in eq 2

$$2CO + 2CH_3ONO \rightarrow (COOCH_3)_2 + 2NO \quad (1)$$

$$2NO + 2CH_3OH + {}^1/_2O_2 \rightarrow 2CH_3ONO + H_2O \quad (2)$$

with the presence of oxygen and methanol, forming methyl nitrite as the feed to the first reaction at an ambient temperature without catalysts. Combination of eqs 1 and 2 gives eq 3. Dimethyl carbonate (DMC) is the main byproduct produced by eq 4.

$$2CO + 2CH_3OH + {}^1/_2O_2 \rightarrow (COOCH_3)_2 + H_2O \quad (3)$$

$$CO + 2CH_3ONO \rightarrow CO(OCH_3)_2 + 2NO \quad (4)$$

Various supported palladium catalysts for gas-phase synthesis of DMO have been investigated, and the results have demonstrated that higher conversion and selectivity are realized on $Pd/\alpha\text{-}Al_2O_3$ compared to Pd on active carbon and $\gamma\text{-}Al_2O_3$.[4] Kinetic studies have shown that adsorption of carbon monoxide is the rate-determining step.[7] However, it is difficult to create and maintain a relatively high dispersion of the active phase on α-alumina of low surface area. In addition, an increasing demand of glycol prompts the development of new catalysts and processes for production of oxalacetic esters.

Due to the unique chemical and physical properties, the syntheses and applications of carbon nanofibers have received increasing interest.[8−13] Carbon nanofibers can be catalytically synthesized by decomposition of various hydrocarbons or CO on the surface of Ni, Fe, or Co or their alloys either as a metallic powder or as a supported catalyst. De Jong and Geus have reviewed catalytic synthesis of carbon nanofibers and their application as the catalyst support.[10] Ledoux and coworkers have also recently reviewed applications of carbon nanomaterials as catalysts and catalyst supports.[13] The peculiar structures and properties make carbon nanofibers promising candidates as catalysts and catalyst supports. Carbon nanofiber supported catalysts have been investigated in several important reaction systems.[14−20] It has been found that the large specific area and special configuration of graphite edges on the carbon nanofiber surface, combined with its good electronic conductivity, make the carbon nanofiber supported catalysts more active and selective.[12−20]

In this paper we present the preparation and characterization of carbon nanofibers of different nanostrutures. The work also deals with the preparation and characterization of carbon nanofiber supported palladium catalysts, which are tested in the gas-phase synthesis of dimethyl oxalate. The effects of carbon

* To whom correspondence should be addressed. Tel.: 86-21-6425 2884. Fax: 86-21-6425 3528. E-mail: wkyuan@ecust.edu.cn.

[†] East China University of Science and Technology.

[‡] Norwegian University of Science and Technology.

10.1021/ie030728z CCC: $27.50
Published on Web 05/28/2004

nanostructure and functionalization methods on catalyst properties are discussed. A comparison between these new catalysts and conventional catalysts such as Pd/α-Al_2O_3 and Pd/γ-Al_2O_3 is presented.

Experimental Section

Catalytic Synthesis of Carbon Nanofibers. Carbon nanofibers are synthesized on 20 wt % Ni/γ-Al_2O_3 and 20 wt % NiFe (1:1)/γ-Al_2O_3. A deposition−precipitation method is used to prepare finely dispersed metal catalysts. Details of the preparation procedures were described by Geus[21] and Hoogenraad.[22] After injection of the diluted solution containing the active component precursor, the subsequent precipitate is filtered, washed, dried overnight at 120 °C, and then calcined in stationary air for 5 h at 600 °C.

Typically 1.0 g of catalyst is loaded in a quartz reactor mounted in a horizontal tubular furnace. The sample is initially reduced in a 25% hydrogen−argon stream at 600 °C for 3 h. Following this step, a desired mixture of carbon monoxide/hydrogen (4:1) is led into the reactor and the reaction is allowed to proceed for a period of 16 h. All the gas flow rates are measured by mass flow controllers. Gas effluents are analyzed by GC. Each run produces more than 10 g of carbon nanofibers.

Oxidation of carbon nanofibers has been conducted to introduce surface functional groups. To study the effects of functionaliztion of the catalyst properties, both air and HNO_3 have been used as oxidants. Part of the as-grown carbon nanofibers can be subsequently oxidized overnight in the air at 400 °C. The rest of the as-grown carbon nanofibers are subsequently soaked in a 4 M nitride acid aqueous solution for 6 days, then filtered, thoroughly washed in deionized water, and dried overnight at 120 °C.

Preparation of Carbon Nanofiber Supported Pd Catalysts. Supported catalysts containing 1 wt % palladium are prepared by an incipient wetness impregnation method with an aqueous solution containing $PdCl_2$ and HCl. The wet solid is dried at 80 °C overnight and then calcined in stationary air at a temperature of 350 °C for 5 h. The resulting dry solid is reduced under flowing pure hydrogen at 350 °C for 5 h. The samples are cooled in the presence of argon to room temperature and are then stored in a sealed vessel. For Pd/γ-Al_2O_3 and Pd/α-Al_2O_3 catalyst preparation, similar procedures are followed except for carrying out the calcination and the reduction for 16 h.[23]

Catalyst Characterization. Surface area and textual properties of the supports are measured by nitrogen adsorption at 77.4 K with a Micromeritics ASAP 2010 apparatus. The samples are degassed for 5 h at 190 °C, prior to the measurements.

The microstructure and the morphology of various supports and supported palladium catalysts are studied using a JEOL JEM 2010 transmission electron microscope with an accelerating voltage of 200 kV and a lattice resolution of 0.18 nm. Suitable transmission specimens are prepared by ultrasonic dispersion of the respective samples in ethanol, followed by dropping the suspension onto a holey carbon-coated copper grid.

Metal dispersions are measured using a CO pulse chemisorption procedure in a Micromeritics AutoChem (II) apparatus. The weighted catalysts are directly reduced in the mixture of 10% H_2/Ar at a temperature of 150 °C for 30 min and then degassed by helium for 20 min at 150 °C. After the catalysts are cooled to the temperature of 35 °C on the helium flow, the carbon monoxide pulses are injected into the quartz reactor and the net volume of CO is recorded by TCD. The chemisorption stoichiometry of one CO molecule per surface palladium atom is assumed.

Catalyst Activity Test for DMO Synthesis. Catalytic studies are performed in a quartz reactor where the catalyst sample (1.80 g) is packed at a fixed bed. The gas reactant, composed of 10% (v/v) methyl nitrite and 90% nitrogen, is generated through a reaction between sodium nitrite and methanol as shown in eq 5. As the mixture of sodium nitrite and methanol is

$$2NaNO_2 + 2CH_3OH + H_2SO_4 \rightarrow 2CH_3ONO + Na_2SO_4 + 2H_2O \quad (5)$$

vigorously stirred in a vessel, concentrated H_2SO_4 is slowly dropped in to carry out the reaction, and a CH_3ONO-containing effluent is collected. The ratio of both gases (CH_3ONO and N_2) is controlled by the partial pressure of CH_3ONO, allowing a constant composition of desired reactant. The catalyst sample is reduced in a hydrogen and nitrogen mixture (25% H_2) at 350 °C for several hours, and the temperature is then lowered to 120 °C for synthesis of DMO. The gas reactant consisting of methyl nitrite (mixed with nitrogen) and carbon monoxide is led into the reactor at a CH_3ONO:CO:N_2 molar ratio of 1:1.25:9. The flow rate of carbon monoxide remains at 15 mL/min, and the reaction lasts for 120 min. The concentration of methyl nitrite is determined by GC (HP5890) equipped with a TDX-1-packed column. After reaction, the collected solid is dissolved in methanol; the solution is also analyzed using a GC instrument (HP5890) equipped with an OV-101 column to determine the DMO purity.

Results and Discussion

Characterizations of Carbon Nanofibers. From the TEM images (Figure 1a,c) of the as-grown carbon nanofibers, metal particles and alumina support can also be observed, while the metal particles are removed by treating the carbon nanofibers in a HNO_3 solution as shown in Figure 1b,d. By examining these images, one may appreciate that the diameter distribution of the carbon nanofibers is relatively narrow and that the diameter of the formed carbon nanofibers is almost less than 50 nm. This is possibly due to a fine dispersion of metal particles on the support, since it is well-known that the deposition−precipitation method can yield small particles with a narrow distribution. However, when the metal powder is used as the catalyst, the diameter of the produced carbon nanofiber is larger and the distribution is wider. This phenomenon is in good agreement with the observation in the literature.[24]

During further HRTEM studies some very interesting features have been observed concerning the influence of the catalyst composition on the nanostructure of carbon nanofibers generated from the CO/H_2 (4:1) mixture at 600 °C. In Figure 2a, the orientation of the graphite platelets is aligned in a direction parallel to the fiber axis and some defects are also observed, defined as CNF-00 (the angle between graphite platelet e and the axis of the carbon nanofiber is 0). These defects appear as a bamboo-like structure, indicating some breakage of the tubular carbon nanofiber growth. This phenomenon can possibly be linked to reconstruction of the metal particles during the catalytic growth

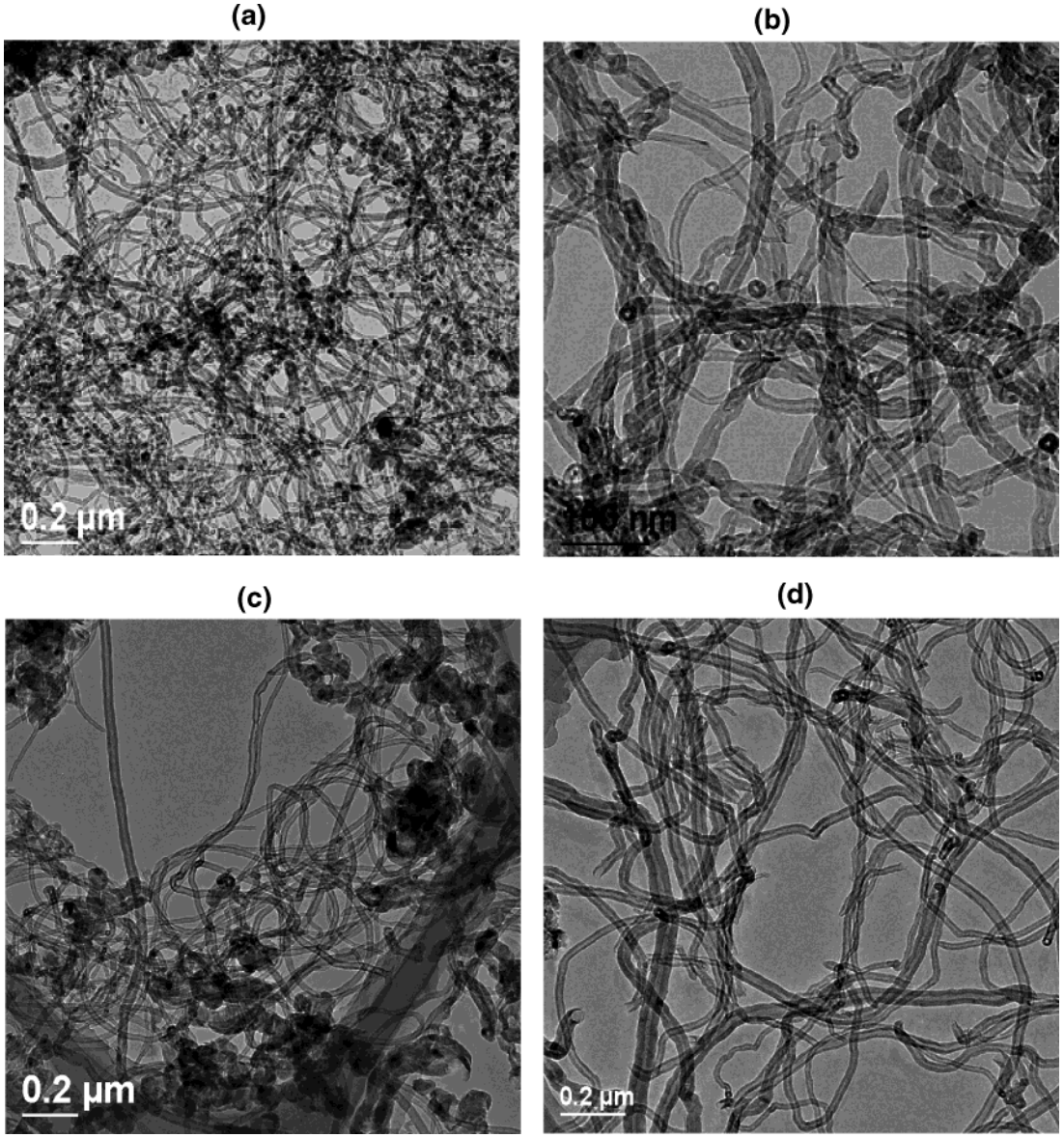

Figure 1. (a, top left) TEM image of the fresh carbon nanofibers produced by disproportionation of CO on 20% Ni/Al_2O_3 (CNF-00) at the conditions $CO:H_2 = 4:1$, $P_{tot} = 1$ bar, and $T = 600$ °C. (b, top right) TEM image of the carbon nanofibers after treatment in HNO_3 solution produced by disproportionation of CO on 20% Ni/Al_2O_3 (CNF-00−HNO_3) at the conditions $CO:H_2 = 4:1$, $P_{tot} = 1$ bar, and $T = 600$ °C. (c, bottom left) TEM image of the fresh carbon nanofibers produced by disproportionation of CO on 20% NiFe (1:1)/Al_2O_3 (CNF-05) at the conditions $CO:H_2 = 4:1$, $P_{tot} = 1$ bar, and $T = 600$ °C. (d, bottom right) TEM image of the carbon nanofibers after treatment in HNO_3 solution produced by disproportionation of CO on 20% NiFe (1:1)/Al_2O_3 (CNF-05−HNO_3) at the conditions $CO:H_2 = 4:1$, $P_{tot} = 1$ bar, and $T = 600$ °C.

process. It has been revealed that carbon nanofiber formation involves surface reactions leading to surface carbon formation on the gas−metal interface. The formed carbon segregates, diffuses, and precipitates on the back of the metallic particles.[25] The carbon concentration in the particles is determined by a balance between the surface reaction and diffusion of carbon through the particle. When the surface reaction rate is faster than the diffusion rate, the carbon site coverage and the carbon concentration as well will increase with time. As a consequence, the Ni lattice is expanded and the Ni−Ni bond length increases when a relatively high amount of carbon is inserted into the lattice, since the nickel atom has a covalent radius of 1.15 Å compared to carbon having a covalent radius of 0.77 Å. It implies that accumulation of carbon atoms in the Ni crystal destabilizes the lattice, and creates some driving force for reconstruction of Ni crystals. At a certain carbon concentration, the crystal will instantly release carbon onto the back of the Ni particle.

However, the defected nanostructure of carbon nanofibers produced on the NiFe (1:1)/Al_2O_3 catalyst is not clearly observed in a typical image (Figure 2b). The graphite platelets are not completely parallel to the axis of carbon nanofibers, and there is a small angle apart from the axis, about 5−10° (CNF-05). Anyhow, the angle is so small that the structure is very close to that of a carbon nanotube. The difference in nanostructure of different catalysts can possibly be explained by the crystallographic orientation on the active metal particle faces.

The measured surface area and pore volumes of different samples are shown in Table 1. The surface areas of carbon nanofibers are high and close to that of γ-Al_2O_3. The measured surface area of α-Al_2O_3 is very low as expected. It is found that the surface area of the

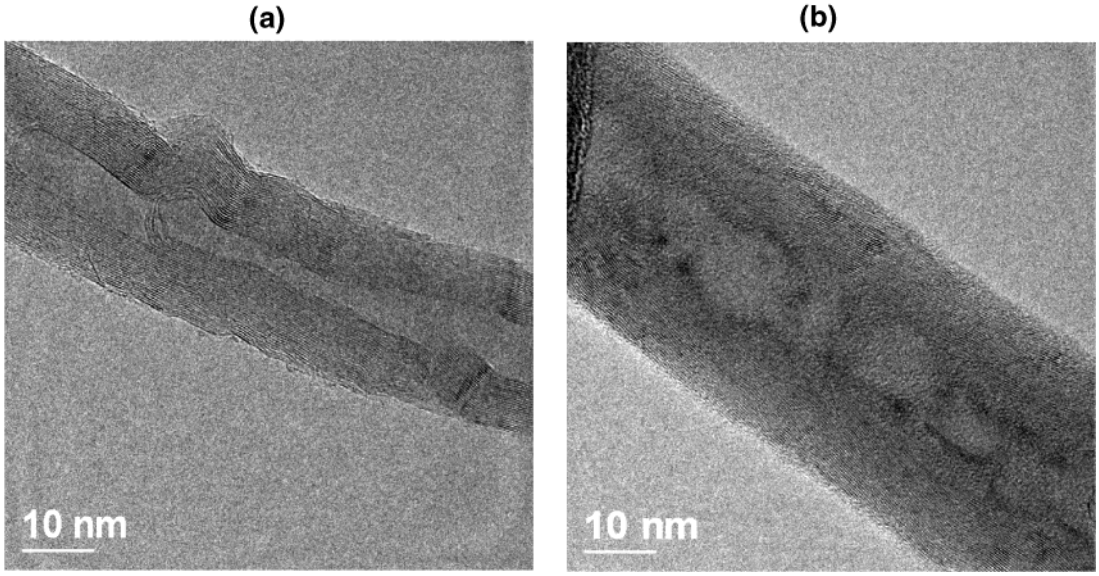

Figure 2. (a, left) HRTEM image of carbon nanofibers produced by disproportionation of CO on 20% Ni/Al_2O_3 (CNF-00) at the conditions $CO:H_2 = 4:1$, $P_{tot} = 1$ bar, and $T = 600$ °C. (b, right) HRTEM image of carbon nanofibers produced by disproportionation of CO on 20% NiFe (1:1)/Al_2O_3 (CNF-05) at the conditions $CO:H_2 = 4:1$, $P_{tot} = 1$ bar, and $T = 600$ °C.

Table 1. Texture of Various Supports and Dispersion of Supported Palladium Catalysts

					CO chemisorption	
support[a]	structure[b]	BET surface area (m^2/g)	micropore vol (cm^3/g)	total pore vol (cm^3/g)	dispersion (%)	diameter (nm)
α-alumina		15.5	0.000	0.108	6.70	16.7
γ-alumina		211.1	0.002	0.443		
CNF-00−air	CNF-00	139.4	0.007	0.273	27.38	4.34
CNF-00−HNO_3	CNF-00	130.9	0.006	0.291	26.54	4.48
CNF-05−air	CNF-05	170.0	0.008	0.388	29.31	4.05
CNF-05−HNO_3	CNF-05	161.9	0.007	0.375	27.11	4.38

[a] CNF-00 and CNF-05 indicate that carbon nanofibers (CNFs) are produced from disproportionation of CO on 20 wt % Ni/Al_2O_3 and on 20 wt % NiFe (1:1)/Al_2O_3, respectively. Air and HNO_3 indicate the oxidant used in functionalization. [b] CNF-00 and CNF-05 indicate that the angle between the graphite platelet and the axis of the carbon nanofiber is 0 and 5°, respectively.

carbon nanofiber produced on 20 wt % $NiFe/Al_2O_3$ is larger than that on 20% Ni/Al_2O_3. Formation of the larger surface area can be explained by the fact that there must be more graphite edge exposed to the surface of CNF-05 compared to that of CNF-00. Although oxidation in air yields slightly higher surface area and larger pore volume than in HNO_3, no significant effects on surface area using different oxidants have been observed. The difference is only about 8 m^2/g.

Characterization of Supported Palladium Catalysts. The size and distribution of palladium particles on different supports have been investigated by HR-TEM. Only palladium supported on carbon nanofibers with functionalization in air are selected for TEM studies, and the results are also compared to those for palladium supported on α-alumina (see Figure 3a−c). The TEM images (Figure 3) show that palladium particles on α-alumina (Figure 3a) are larger than 10 nm, while the palladium particles on carbon nanofiber supports (Figure 3b,c) present a much smaller size: most palladium particles are smaller than 5 nm, and the particle size distribution is relatively narrow. Similar particle sizes are observed on CNF-00 (Figure 3b) and on CNF-05 (Figure 3c), probably due to their similar carbon nanostructures as discussed above. Furthermore, metal dispersions and the average diameter of palladium particles measured by the CO pulse chemisorption method are in agreement with the examined TEM results as shown in Table 1. The high dispersion of the metal particles could be attributed to high surface area and the specific features of the surface of the carbon nanofibers.[26,27] The surface ratio of basal and edge planes can be deliberately controlled by selecting the growth condition; therefore, carbon nanofiber based catalysts can be prepared intentionally to achieve some desired properties. Particularly, steps or terraces on the surface of a small-diameter carbon nanofiber might benefit anchoring of the active component precursor, and thus help to disperse the palladium particles very finely on the support.

On the other hand, the surface of as-grown carbon nanofibers is hydrophobic due to the existence of basal planes of graphite platelets. This extremely valuable advantage for a common inert substrate consequently has a weak point in that the active component precursor is difficult to anchor on the surface. Functionalization of the surface to introduce oxygen-containing groups by the oxidant is an essential step in application of carbon nanofibers. Oxygen-containing groups are considered as anchoring sites for favoring a higher dispersion of the metal. Mojet and Hoogerraad[28] studied the preparation of carbon nanofiber supported palladium catalysts using an ion-exchange technique and found that the palladium ions interacted directly with the basal plane. Moreover, Simonov[29] has done extensive research on H_2PdCl_4 produced in aqueous solution adsorbed on the surface of a graphite-like carbon material and also found that there was weak interaction between the basal plane and the active phase, but no direct interaction of the Pd(II) complex and oxygen-containing groups. According to

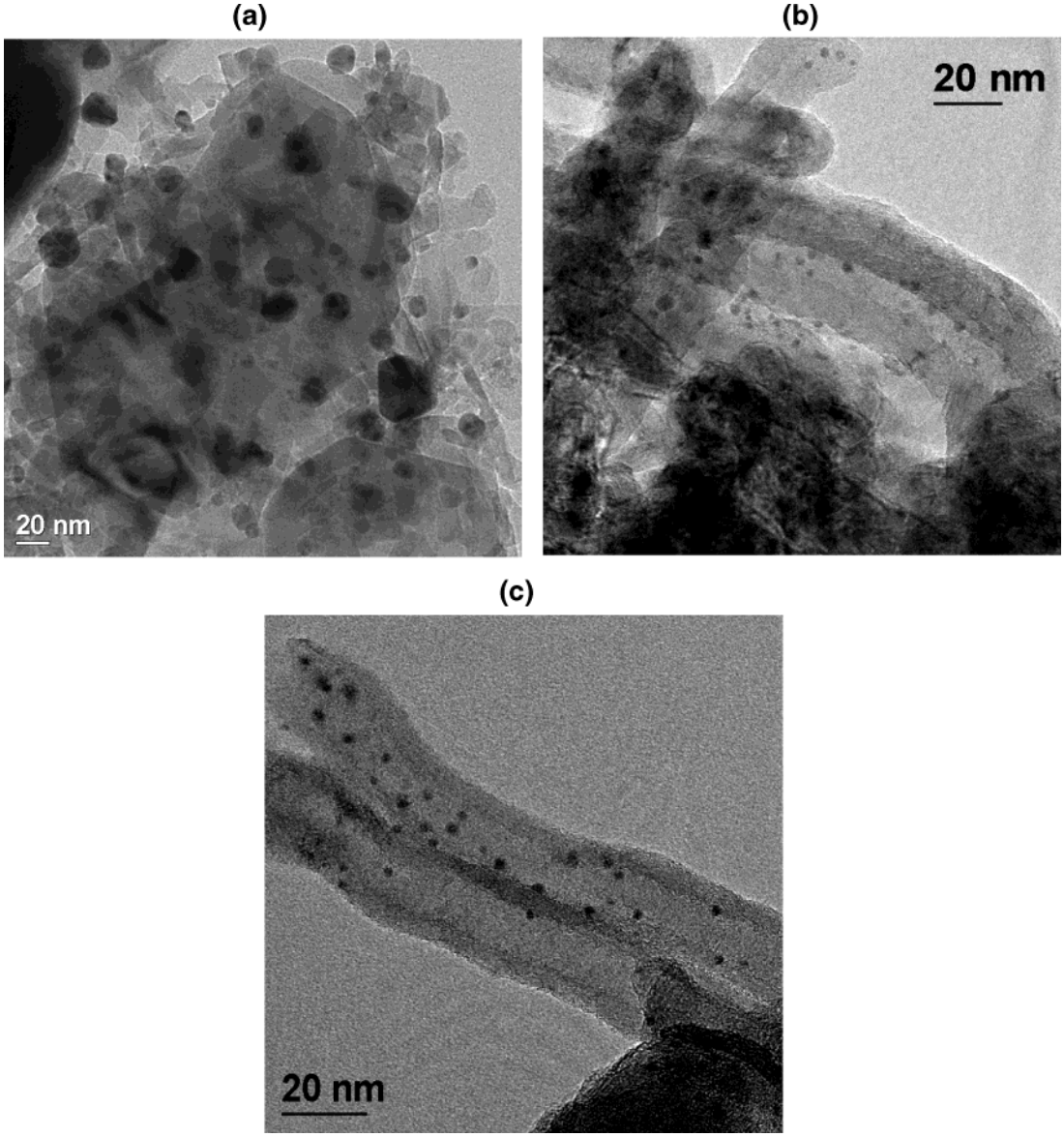

Figure 3. (a, top left) TEM images of α-alumina supported palladium particles: 1 wt % Pd/α-Al_2O_3. (b, top right) TEM images of CNF-00−HNO_3 supported palladium particles: 1 wt % Pd/CNF-00−air. (c, bottom) TEM images of CNF-05−HNO_3 supported palladium particles: 1 wt % Pd/CNF-05−air.

this point, the functionlization of the carbon nanofiber surface makes CNFs more hydrophilic, and they thus benefit from impregnation and stabilization of the active phase.[30]

Catalyst Activity Test. According to thermodynamic analysis, the reaction shown as eq 2 can be regarded as an irreversible one.[7] The reaction of a CO and CH_3ONO (1.25:1) mixture is performed on the various supported palladium catalysts at 120 °C. Analysis of the CH_3ONO concentration is done once every 30 min. In most cases, the reaction reaches a steady state after 10 min. The conversion of CH_3ONO is found to be strongly dependent upon the nature of the support material as shown in Figure 4. Inspection of these results indicates that Pd/CNF-05 after oxidation treatment in the air offers the highest activity, resulting in a CH_3ONO conversion at 85%. The activities of palladium catalysts on different supports can be arranged as follows:

CNF-05−air > CNF-05−HNO_3 > CNF-00−air (CNF-00−HNO_3) > α-Al_2O_3 > γ-Al_2O_3

It was previously reported in the literature that the conversion of methyl nitrite on Pd/γ-Al_2O_3 was lower than on Pd/α-Al_2O_3.[4] Uchumi[4] concluded that α-Al_2O_3 and activated carbon were more preferable supports than γ-Al_2O_3 for the gas-phase synthesis of DMO, although the function of the support had not been well understood. A redox reaction mechanism has been generally accepted to explain the reaction. As mentioned above, the crucial step in this catalytic process is the redox step between Pd(0) and Pd(II) to form a catalytic cycle. The needs for reoxidation or reduction depend on the reaction nature. Experimental results show that Pd(0) catalyzes the formation of DMO (eq 2) (forming reaction) while Pd(II) catalyzes the formation of DMC (eq 4).[31] The key step in the redox mechanism can simply be expressed as

$$\mathrm{Pd(0)} \underset{\mathrm{CO}}{\overset{\mathrm{CH_3ONO}}{\rightleftharpoons}} \mathrm{Pd(II)} \qquad (6)$$

Methyl nitrite oxidizes palladium, while CO reduces Pd(II). The interaction between Pd(0)/Pd(II) and the sup-

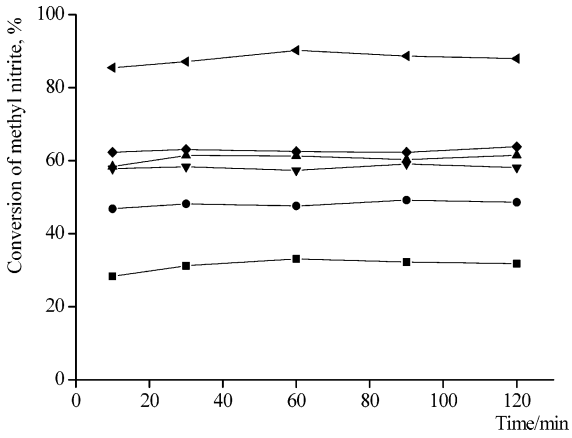

Figure 4. Conversion of methyl nitrite as a function of time on stream at 120 °C and a $CH_3ONO:CO:N_2$ molar ratio of 1:1.25:9 on the various supported 1 wt % palladium catalysts: (■) 1% Pd/γ-Al_2O_3; (●) 1% Pd/α-Al_2O_3; (▼) 1% Pd/CNF-00−HNO_3; (▲) 1% Pd/CNF-00−air; (◆) 1% Pd/CNF-05−HNO_3; (rotated ▲) 1% Pd/CNF-05−air.

port seems to play a significant role in the redox properties of the catalysts.

It is expected that interaction of the palladium particles supported on α-Al_2O_3 is much weaker than on γ-Al_2O_3. The strong interaction might suppress both oxidation of Pd(0) to Pd(II) and reduction from Pd(II) to Pd(0), and thus should result in a lower activity. This assumption is supported by the fact that Pd/SiO_2 is more active than Pd/γ-Al_2O_3, since it is expected that SiO_2 yields much lower metal−support interaction than γ-Al_2O_3. However, the low surface area is the major drawback for using α-Al_2O_3 as the catalyst support. On the basis of this analysis, an ideal catalyst for this reaction should be of high surface area but relatively low metal−support interaction.

As discussed above, the strong metal−support interaction results in a lower reduction/oxidation potential of the palladium particle surface, and thus in lower activity. CNF-05 and CNF-00 combine the advantages of α-Al_2O_3, namely, weak metal−support interaction, and of activated carbon, namely, high surface area. The higher activity using CNF-05-HNO_3 compared with CNF-00-HNO_3 may be explained by a slightly higher surface area of CNF-05, as shown in Table 1. The difference in the surface structure between carbon nanofibers and α-Al_2O_3 may also explain why the former provides higher activity. Halls and co-workers[32] studied the potential role of carbon monoxide in the gas-phase catalytic growth of carbon nanotubes using the semiempirical direct dynamic simulation method and found that carbon monoxide adsorption onto the nanotube edges was kinetically and thermodynamically favored. Chen[7] and Luo[33] investigated the intrinsic kinetics of dimethyl oxalate synthesis on α-alumina supported palladium catalysts and showed that the rate-determining step of the reaction (eq 1) was adsorption of carbon monoxide. Hence, enhanced adsorption of carbon monoxide may also contribute to the higher performance of carbon nanofibers than α-Al_2O_3.

Another important finding in the present work is that functionalization of carbon nanofibers has significant effects on the performance of the palladium catalysts. Figure 4 indicates that palladium deposited on a carbon nanofiber functionalized by air prevails over that deposited on a carbon nanofiber treated in HNO_3. However, the difference in activity caused by different means of oxidation treatment of CNF-05 cannot simply be explained by their difference in surface area. The surface area of CNF-05 treated in air results only in a 5% increase compared to that of CNF-05 treated in HNO_3, but the activity increased about 38%. It is interesting to point out that such a significant effect caused by different oxidants cannot be observed in the case of CNF-00 produced from CO/H_2 on Ni catalysts. An important difference between air and HNO_3 functionaliztion is that metal particles, such as Ni and NiFe particles, that should be removed when treated by HNO_3 remain on the carbon nanofibers when treated by air. The remaining particles can dissolve in the HCl and $PdCl_2$ solutions during impregnation, and deposit again on the surface. Ni and NiFe can then serve as a promoter. However, the significant activity increase is only for the NiFe catalyst, and not for the Ni catalyst, indicating that the Fe (ion) might be an effective promoter for the DMO synthesis. This might imply that the high activity of the CNF-05 supported palladium catalyst prepared in the CO/H_2 mixture on NiFe/γ-Al_2O_3 can be attributed to the high surface area, weak metal−support interaction, and Fe promoting effects. Recently, Xu and Meng have investigated the kinetics of the catalytic reaction carbon monoxide to diethyl oxalate over Pd−Fe/α-alumina.[34] It is implied that the iron (ion) promotes the synthesis of DMO on the α-alumina supported palladium catalysts in agreement with the results on carbon nanofibers in the present work.

Table 2. Effect of the Support on the Selectivity (%) in the Synthesis of DMO at 120 °C

support[a]	structure[b]	DMO	DMC
α-alumina		96.1	3.9
γ-alumina		93.8	6.2
CNF-00−air	CNF-00	99.0	1.0
CNF-00−HNO_3	CNF-00	98.7	1.3
CNF-05−air	CNF-05	99.0	1.0
CNF-05−HNO_3	CNF-05	98.8	1.2

[a] CNF-00 and CNF-05 indicate that carbon nanofibers (CNFs) are produced from disproportionation of CO on 20 wt % Ni/Al_2O_3 and on 20 wt % NiFe (1:1)/Al_2O_3, respectively. Air and HNO_3 indicate the oxidant used in functionlization. [b] CNF-00 and CNF-05 indicate that the angle between the graphite platelet and the axis of the carbon nanofiber is 0 and 5°, respectively.

Besides the significant improvement in the activity of Pd/CNF, an improvement in the selectivity to DMO has also been observed using carbon nanofiber supports, as shown in Table 2. As was reviewed by Uchiumi et al.[4] the selectivity to DMO seems to depend on the acidity of the support. Lower acidity seems to be favorable for DMO synthesis. It is found that the selectivity to DMO is about 96% on α-Al_2O_3, while it is more than 98% with CNF−air supports. Characterization of the carbon nanofiber reveals that the surface is of redox-amphoteric character. It can be concluded that such a feature increases the selectivity of DMO.

Conclusions

Carbon nanofibers have been synthesized by disproportionation of CO in the presence of hydrogen on 20 wt % Ni/γ-Al_2O_3 and 20 wt % NiFe (1:1)/γ-Al_2O_3 with relatively high yields at 600 °C. The deposition−precipitation method yields highly dispersed Ni and NiFe particles on γ-Al_2O_3. HRTEM studies provide some key insights into the morphological characteristics of carbon nanofibers and of the palladium particles on the support. CNF-00 has been synthesized on Ni/γ-Al_2O_3,

and CNF-05 has been synthesized on NiFe (1:1)/γ-Al_2O_3. Palladium particles are homogeneously deposited on the outer edges of the carbon nanofibers by the standard incipient wetness impregnation method, and also on γ-alumina and α-alumina supports. The diameter of the palladium particles of the carbon nanofiber supported catalyst is mainly less than 5 nm, which is much smaller than those on α-alumina. Finely dispersed palladium particles on carbon nanofibers are explained by the high surface area and oxygen-containing groups on the surface.

Carbon nanofibers as supports result in a significant improvement in the gas-phase synthesis of dimethyl oxalate compared to the alumina supported catalyst. Experimental results show that palladium supported on CNF-05 funtionalized by air oxidation offers the highest activity for DMO synthesis. A small metal particle size and relatively low metal−support interaction can enhance the redox properties. Enhanced carbon monoxide adsorption and possible Fe promotion effects are factors that have been proposed to explain the high activity and selectivity over carbon nanofiber based catalysts.

Acknowledgment

This work was done under the support of the National Science Foundation of China and the Development Project of Shanghai Priority Academic Discipline.

Literature Cited

(1) Nakamura, A.; Matsuzaki, T. A New Oxidation System Using Nitrite Oxidatants. *Res. Chem. Intermed.* **1998**, *26*, 213.

(2) Wang, J.; Ma, X.; Han, S.; Xu, G. Preparation of Diethyl Oxalate by CO Coupling Reaction in a Gas-solid Fixed Bed Reactor. *J. Nat. Gas Chem.* **2000**, *9*, 319.

(3) Jiang, X.; Su, Y.; Lee, B.; Chien, S. A Study on the Synthesis of Diethyl Oxalate over Pd/α-Al_2O_3 Catalysts. *Appl. Catal., A* **2001**, *211*, 47.

(4) Uchiumi, S.; Ataka, K.; Matsuzaki, T. Oxidative Reactions by a Palladium-Alkyl Nitrite System. *J. Organomet. Chem.* **1999**, *576*, 279.

(5) Matsuzaki, T.; Nakamura, A. Dimethyl Carbonate Synthesis and Other Oxidative Reaction Using Alkyl Nitrites. *Catal. Surv. Jpn.* **1997**, *1*, 77.

(6) Huo, Z.; Li, Z.; Wang, B.; Ma, X.; Xu, G. Influence of Support Properties on CO Vapor-Phase Catalytic Coupling Reactions. *Chem. React. Eng. Technol.* **2002**, *18*, 31 (in Chinese).

(7) Ma, X.; Xu, G.; Chen, J.; Chen, H. Kinetics Carbon Monoxide Catalytic Coupling to Ethyl Nitrite in Gaseous Phase. *J. Chem. Ind. Eng.* **1995**, *46*, 50 (in Chinese).

(8) Iijima, S. Helical Microtubules of Graphitic Carbon. *Nature* **1991**, *354*, 56.

(9) Rodriguez, N. M. A Review of Catalytically Grown Carbon Nanofibers. *J. Mater. Res.* **1993**, *8*, 3233.

(10) De Jong, K. P.; Geus, J. W. Carbon Nanofibers: Catalytic Synthesis and Applications. *Catal. Rev.—Sci. Eng.* **2000**, *42*, 481.

(11) Rodriguez, N. M.; Chambers, A.; Baker, R. T. K. Catalytic Engineering of Carbon Nanostructures. *Langmuir* **1995**, *11*, 3862.

(12) Hoogenraad, M. S.; van Leeuwarden, R. A. G. M.; van Breda Vriesman, G. J. B.; Broersma, A.; van Dillen, A. J.; Geus, J. W. *Stud. Surf. Sci. Catal.* **1995**, *91*, 263.

(13) Ledoux, M. J.; Vieira, R.; Pham-Huu, C.; Keller, N. New Catalytic Phenomena on Nanostructured (Fibers and Tubes) Catalysts. *J. Catal.* **2003**, *216*, 333.

(14) Planeix, J. M.; Coustel, N.; Coq, B.; Brotons, V.; Kumbhar, P. S.; Dutartre, R.; Geneste, P.; Bernier, P.; Ajayan, P. M. Application of Carbon Nanotubes as Supports in Heterogeneous Catalysis. *J. Am. Chem. Soc.* **1994**, *116*, 7935.

(15) Chambers, A.; Nemes, T.; Rodriguez, M. N.; Baker, R. T. K. Catalytic Behaviour of Graphite Nanofiber Supported Nickel Particles. 1. Comparison with Other Support Media. *J. Phys. Chem. B* **1998**, *102*, 2251.

(16) Park, C.; Baker, R. T. K. Catalytic Behaviour of Graphite Nanofiber Supported Nickel Particles. 2. The Influence of the Nanofiber Structure. *J. Phys. Chem. B* **1998**, *102*, 5168.

(17) Chambers, A.; Baker, R. T. K. Catalytic Behaviour of Graphite Nanofiber Supported Nickel Particles. 3. The Effect of Chemical Blocking on the Performance of the System. *J. Phys. Chem. B* **1999**, *103*, 2454.

(18) Gao, R.; Tan, C. D.; Baker, R. T. K. Ethylene Hydroformylation on Graphite Nanofiber Supported Rhodium Catalysts. *Catal. Today* **2001**, *65*, 19.

(19) Ros, T. G. Rhodium Complexes and Particles on Carbon Nanofibres. Ph.D. Dissertation, Utrecht University, Utrecht, The Netherlands, 2002.

(20) Zhang, Y.; Zhang, H.; Lin, G.; Chen, P.; Yuan, Y.; Tsai, K. R. Preparation, Characterization and Catalyic Hydroformylation properties of Carbon Nanotubes-supported Rh-phosphine Catalyst. *Appl. Catal., A* **1999**, *187*, 213.

(21) Boellaard, E.; van der Karaan, A. M.; Geus, J. W. Preparation of Supported Mono- and Bimetallic Catalysts by Deposition-precipitation of Metal Cyanide Complexes. *Stud. Surf. Sci. Catal.* **1995**, *91*, 931.

(22) Hoogenraad, M. S.; Onwezen, M. F.; van Dillen, A. J.; Geus, J. W. *Stud. Surf. Sci. Catal.* **1994**, *101*, 1331.

(23) Geus, J. W.; van Veen, J. A. R. Preparation of Supported Catalysts. *Stud. Surf. Sci. Catal.* **1993**, *79*, 459.

(24) Park, C.; Rodriguez, N. M.; Baker, R. T. K. Carbon Deposition on Iron-Nickel during Interaction with Carbon Monoxide−Hydrogen Mixtures. *J. Catal.* **1997**, *169*, 212.

(25) Hoogenraad, M. S. Growth and Ultilization of Carbon Fibrils. Ph.D. Dissertation, Utrecht University, Utrecht, The Netherlands, 1995.

(26) Toebes, M. L.; van Dillen, J. A.; de Jong, K. P. Synthesis of Supported Palladium Catalysts. *J. Mol. Catal. A* **2001**, *173*, 75.

(27) Likholobov, V. A. Catalysis by Novel Carbon-based Materials. In *Catalysis by Unique Metal Ion Structures in Solid Matrics*; Centi, G., et al., Eds.; Kluwer Academic Publishers: Dordrecht, The Netherlands, 2001.

(28) Mojet, B. L.; Hoogenraad, M. S.; van Dillen, J. A.; Geus, J. W.; Koningsberger, D. C. *J. Chem. Soc., Faraday Trans.* **1997**, *93* (24), 4371.

(29) Simonov, P. A.; Romanenko, A. V.; Prosvirn, I. P.; Moroz, E. M.; Bornin, A. I.; Chuvilin, A. L.; Likholobov, V. A. On the Nature of the Interaction of H_2PdCl_4 with the Surface of Graphite-like Carbon Materials. *Carbon* **1997**, *35*, 73.

(30) Schoegl, R. Carbons. In *Preparation of Solid Catalysts*; Ertl, G., Knoezinger, H., Weitkamp, J., Eds.; Wiley-VCH: Weinheim, Germany, 1999.

(31) Pawlow, J. H.; Sadow, A. D.; Sen, A. Palladium(II)-Catalyzed Terpolymerization of Alkane-α,ω-Dinitrite Esters, Alkenes, and Carbon Monoxide to Polysuccinates. *Organometallics* **1997**, *16*, 5659.

(32) Mann, D. J.; Halls, M. D.; Hase, W. L. Direct Dynamics Studies of CO-Assisted Carbon Nanotubes Growth. *J. Phys. Chem. B* **2002**, *106*, 12418.

(33) You, Q.; Xu, W.; Luo, Y. Studies of the Kinetics of Synthesizing Diethyl Oxalate by Vapor Phase Catalytic Coupling Carbon Monoxide and Ethyl Nitrite. *J. Zhejiang Univ. [Nat. Sci. Ed.]* **1991**, *25*, 512 (in Chinese).

(34) Meng, F.; Xu, G.; Guo, Q. Kinetics of the Catalytic Coupling Reaction of Carbon Monoxide to Diethyl Oxalate over Pd-Fe/α-Al_2O_3 Catalyst. *J. Mol. Catal. A* **2003**, *201*, 283.

Received for review September 17, 2003
Revised manuscript received February 18, 2004
Accepted February 26, 2004

IE030728Z